UC Irvine
UC Irvine Previously Published Works

Title

Second-Generation Non-Covalent NAAA Inhibitors are Protective in a Model of Multiple Sclerosis

Permalink

https://escholarship.org/uc/item/6tj059dq

Journal

Angewandte Chemie International Edition, 55(37)

ISSN

1433-7851

Authors

Migliore, Marco
Pontis, Silvia
de Arriba, Angel Luis Fuentes
et al.

Publication Date

2016-09-05

DOI

10.1002/anie.201603746

Peer reviewed

Second-Generation Non-Covalent NAAA Inhibitors are Protective in a Model of Multiple Sclerosis

Marco Migliore[+], Silvia Pontis[+], Angel Luis Fuentes de Arriba, Natalia Realini, Esther Torrente, Andrea Armirotti, Elisa Romeo, Simona Di Martino, Debora Russo, Daniela Pizzirani, Maria Summa, Massimiliano Lanfranco, Giuliana Ottonello, Perrine Busquet, Kwang-Mook Jung, Miguel Garcia-Guzman, Roger Heim, Rita Scarpelli,* and Daniele Piomelli*

Abstract: *Palmitoylethanolamide (PEA) and oleoylethanolamide (OEA) are endogenous lipid mediators that suppress inflammation. Their actions are terminated by the intracellular cysteine amidase, N-acylethanolamine acid amidase (NAAA). Even though NAAA may offer a new target for anti-inflammatory therapy, the lipid-like structures and reactive warheads of current NAAA inhibitors limit the use of these agents as oral drugs. A series of novel benzothiazole–piperazine derivatives that inhibit NAAA in a potent and selective manner by a non-covalent mechanism are described. A prototype member of this class (**8**) displays high oral bioavailability, access to the central nervous system (CNS), and strong activity in a mouse model of multiple sclerosis (MS). This compound exemplifies a second generation of non-covalent NAAA inhibitors that may be useful in the treatment of MS and other chronic CNS disorders.*

NAAA is a cysteine hydrolase that catalyzes the biodegradation of PEA and OEA (Figure 1),[1] two lipids that suppress inflammation by activating the ligand-operated transcription factor, peroxisome proliferator-activated receptor-α (PPAR-α).[2] Macrophages and other host defense cells constitutively generate PEA and OEA in amounts that are sufficient to fully engage PPAR-α.[3] This process is halted during inflammation, leading to a decrease in PPAR-α signaling and acceleration of the inflammatory response.[3]
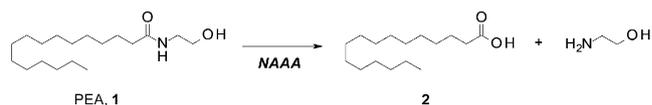
[*] Dr. M. Migliore,[+] Dr. S. Pontis,[+] Dr. A. L. Fuentes de Arriba,
    Dr. N. Realini, Dr. E. Torrente, Dr. A. Armirotti, Dr. E. Romeo,
    Dr. S. Di Martino, Dr. D. Russo, Dr. D. Pizzirani, Dr. M. Summa,
    Dr. M. Lanfranco, Dr. G. Ottonello, Dr. P. Busquet, Dr. R. Scarpelli,
    Prof. D. Piomelli
    Department of Drug Discovery and Development, Fondazione
    Istituto Italiano di Tecnologia
    via Morego 30, 16163 Genoa (Italy)
    E-mail: rita.scarpelli@iit.it
            piomelli@uci.edu

    Dr. M. Garcia-Guzman, Dr. R. Heim
    Anteana Therapeutics
    11189 Sorrento Valley Road, Suite 104, San Diego, CA 92121 (USA)

    Dr. K.-M. Jung, Prof. D. Piomelli
    Departments of Anatomy and Neurobiology, Pharmacology and
    Biological Chemistry, University of California
    Irvine, CA 92697-4625 (USA)

[+] These authors contributed equally to this work.

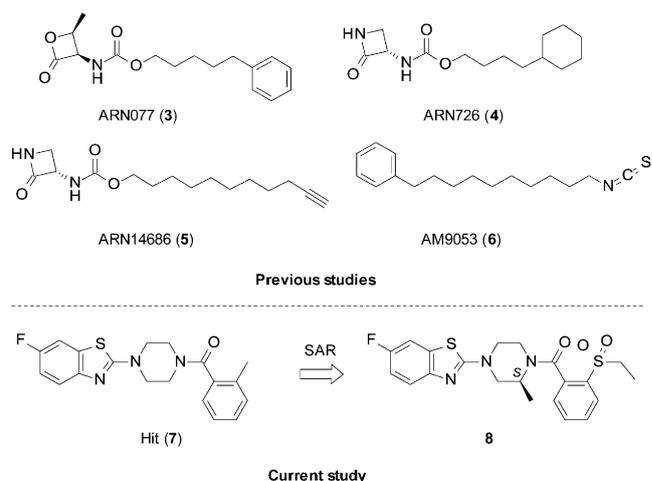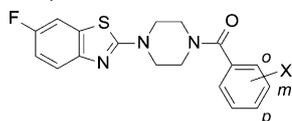   Supporting information for this article can be found under:
    http://dx.doi.org/10.1002/anie.201603746.

Figure 1. NAAA hydrolyzes saturated and monounsaturated fatty acid ethanolamides (for example, PEA (**1**)) into fatty acid (for example, palmitic acid (**2**)) and ethanolamine.

Accordingly, small-molecule NAAA inhibitors restore normal PEA and OEA levels in inflamed tissues and exert marked anti-inflammatory effects in animal models, pointing to NAAA as a potential target for therapy.[4]

Figure 2 illustrates the three most potent classes of NAAA inhibitors described to date. Each class is defined by the presence of a chemical warhead (β-lactone, β-lactam, or isothiocyanate) that can react covalently with the catalytic cysteine of NAAA to form a thioester bond.[5] While potent and, in some cases, systemically active, these molecules share two features that limit their use as oral drugs: 1) the presence of a reactive warhead lowers their metabolic stability (for example, β-lactone **3**)[6] or increases risk of allergic reactions (for example, β-lactam **4** and isothiocyanate **6**);[7] and 2) the hydrophobic fragment that ensures target recognition by these agents negatively impacts drug-likeness.

Herein, we describe a series of benzothiazole–piperazine derivatives that non-covalently inhibit NAAA (Figure 2). Our experiments indicate that compound **8**, a representative

Figure 2. Structures of published NAAA inhibitors (**3**,[6] **4**,[5b] **6**[8]), activity-based NAAA probe (**5**)[9] (top), and compounds reported herein (bottom).

member of this class, is potent, selective for NAAA, and orally available. Moreover, **8** crosses the blood–brain barrier, elevates PEA and OEA levels in the CNS, and is strongly active in a mouse model of MS.

A screening campaign to discover new scaffolds for NAAA inhibition yielded the low-potency hit **7** (Table 1).

Table 1: Inhibitory potencies (IC$_{50}$ in μM) of compounds **7** and **9–16** on the activity of *h*NAAA expressed in HEK-293 cells.
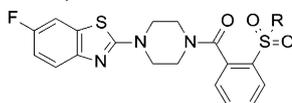

Compound	X	*h*NAAA IC$_{50}$ [μM][a]
7	*o*-CH$_3$	88.9
9	H	NA[b]
10	*o*-Cl	NA
11	*o*-F	NA
12	*o*-OCH$_3$	20.5
13	*o*-SO$_2$CH$_3$	5.69 ± 2.54
14	*o*-SO$_2$CH$_2$CH$_3$	0.45 ± 0.11
15	*m*-SO$_2$CH$_2$CH$_3$	NA
16	*p*-SO$_2$CH$_2$CH$_3$	NA

[a] Values are the mean ± SEM of three or more determinations, or the mean of triplicate determinations in a single experiment. [b] Not Active, <30% inhibition at 100 μM.

To improve potency, we launched a structure–activity relationship (SAR) study that started with the benzamide portion of **7**. Removal of the *o*-methyl group (**9**), or replacement of such a group with a halogen (**10**, **11**), caused a complete loss of activity. By contrast, substitutions with a methoxy (**12**), methylsulfonyl (**13**), or ethylsulfonyl (**14**) group yielded compounds of progressively greater potency. Since moving the ethylsulfonyl substituent to the *meta*- or *para*-position of the phenyl ring strongly reduced activity (**15**, **16**), we focused our exploration on *o*-sulfonyl derivatives containing linear, branched, or cyclic alkyl groups (Table 2). We found that potency was highly sensitive to length and size of the alkyl fragment, with bulkier substituents producing weaker inhibition (for example, **18** and **23**).

Subsequently, we turned to the benzothiazole system, using **14** as an entry point (Table 3). Removal of the 6-F
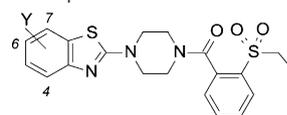
Table 2: Potencies of compounds **17–23** on *h*NAAA.

Compound	R	*h*NAAA IC$_{50}$ [μM][a]
17	(CH$_2$)$_2$CH$_3$	0.39 ± 0.06
18	(CH$_2$)$_3$CH$_3$	8.80 ± 2.40
19	*i*-propyl	0.50 ± 0.09
20	*c*-propyl	0.19 ± 0.03
21	*c*-butyl	0.32 ± 0.00
22	*c*-pentyl	1.10 ± 0.09
23	*c*-hexyl	38.11 ± 5.49

[a] See Footnote for Table 1.

Table 3: Potencies of compounds **24–32** on *h*NAAA.

Compound	Y	*h*NAAA IC$_{50}$ [μM][a]
24	H	0.43 ± 0.03
25	6-Cl	1.55 ± 0.29
26	6-CF$_3$	7.2
27	6-CH$_3$	6.87
28	6-OCH$_3$	5.73
29	4-F	0.55 ± 0.20
30	5-F	2.95 ± 0.84
31	7-F	0.30 ± 0.02
32	7-Cl	0.71 ± 0.21

[a] See Footnote for Table 1.

substituent did not affect potency (**24**), whereas insertion of electron-withdrawing (**25**, **26**) or -donating (**27**, **28**) groups was detrimental. Moving a halogen to various positions of the ring caused either minor effects or a decrease in potency (**29–32**).

The role of the piperazine was probed by replacing it with alternatively oriented piperidines (Table 4). The compounds obtained were either weakly (**33**) or moderately (**34**) active, with **33** being approximately 60 times less potent than **14**. Loss of potency was also observed with **35**, in which a methylene bridge replaces the benzamide carbonyl of **14**. To examine the effect of conformational changes in the piperazine ring, we introduced one or two methyl groups at various positions of this moiety (**36–39**). These attempts did not lead to improvements in potency, but confirmed the role of a mono-substituted piperazine in this region, as shown by the drop in activity caused by 2,2-dimethyl substitution (**38**). Supporting this, we noted that potency was highly sensitive to the configuration of the methyl group, with **40** (the (*R*)-enantiomer of **36**) being 15 times less potent than the (*S*)-enantiomer **8**. Alkyl chain modifications on the sulfonyl substituent of **8** yielded no further improvement (**41** and **42**).

We focused subsequent mechanistic work on **8** because of its greater water solubility, compared to other similarly potent compounds (Table 5; Supporting Information, Table S1). To support this work, an easily scalable synthesis was developed (Scheme 1).

Current NAAA inhibitors react covalently with the catalytic cysteine of NAAA.[5] We used four approaches to probe the interaction of **8** with NAAA. First, we incubated purified human (*h*) NAAA (2 μM) with **8** (50 μM), digested it with trypsin, and searched for covalent adducts using liquid chromatography mass spectrometry (LC-MS). As a positive control, we included the β-lactam **4** (20 μM), for which a covalent interaction with NAAA is documented.[5b] Incubating *h*NAAA with **4** yielded the expected acylated peptide, whereas no such adduct was found when *h*NAAA was exposed to either **8** or vehicle (Figure 3A). Similarly, no covalent adducts were retrieved by a search through the entire peptide map of *h*NAAA (Supporting Information, Figure S1). Second, we incubated *h*NAAA (4.0 μM) with **4** or **8** (1.0 μM), precipitated the protein, and measured compounds in the supernatant by LC-MS. Whereas **4** was

© 2016 Wiley-VCH Verlag GmbH & Co. KGaA, Weinheim

Table 4: Potencies of compounds **8** and **33–42** on *h*NAAA.

Compound	Structure	*h*NAAA IC$_{50}$ [µM][a]
33		26.17 ± 7.15
34		1.77 ± 0.18
35		1.82 ± 0.32
36		0.50 ± 0.075
37		0.72 ± 0.12
38		NA[b]
39		1.44 ± 0.14
40		3.43 ± 0.50
8		0.23 ± 0.04
41		0.20 ± 0.05
42		0.18 ± 0.04

[a, b] See Footnote for Table 1.

Table 5: In vitro metabolism and pharmacokinetic properties of **8** in mice.[a]

Solubility in PBS [µM]	139 ± 1	
Plasma $t_{1/2}$ [min]	> 120[b]	
MLM (NADPH) $t_{1/2}$ [min]	> 60[c]	
MLM (UDPG) $t_{1/2}$ [min]	> 60[d]	
	3 mg kg^{-1} (iv)	3 mg kg^{-1} (oral)
C_{max} [ng mL^{-1}]	1660 ± 166	613 ± 68
T_{max} [min]	(5.0)	30
Cl [mL min^{-1} kg^{-1}]	33.2 ± 1.6	49 ± 8
$t_{1/2}$ [min]	73.9 ± 3.7	104 ± 16
V_d [L kg^{-1}]	3.5 ± 0.2	7.4 ± 1.1
AUC$_{plasma}$ [h×ng mL^{-1}]	1366.8 ± 68.3	988 ± 157
AUC$_{brain}$ [h×ng mL^{-1}]	404.3 ± 109.1	181 ± 28
F [%]	–	72 ± 11

[a] NADPH, reduced nicotinamide adenine dinucleotide phosphate; PBS, phosphate-buffered saline; $t_{1/2}$, terminal half-life; UDPG, uridine diphosphate glucose; AUC, area under the curve; C_{max}, maximal plasma concentration; F%, oral bioavailability; T_{max}, time at which C_{max} is reached. [b] 83 ± 4 % remaining at 120 min; [c] 70 ± 7 % remaining at 60 min; [d] 96 % remaining at 60 min.
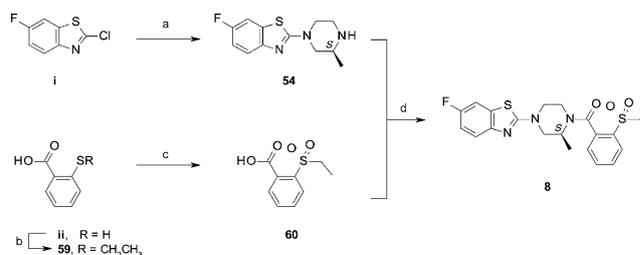
Scheme 1. a) (2S)-2-methylpiperazine, NaHCO$_3$, EtOH/H$_2$O, reflux, 15 h, quantitative; b) EtI, NaOH (2 M), EtOH, RT, 15 h, quantitative; c) oxone, H$_2$O, 40 °C, 15 h, 96 %; d) HATU, Et$_3$N, CH$_3$CN, RT, 15 h, 43 %.

precipitated with NAAA, as expected from its covalent binding to the enzyme, **8** was entirely recovered in the supernatant (Figure 3 B). Third, we investigated whether **8** prevents the binding of the covalent activity-based probe **5** to NAAA.[9] As previously shown,[9] **5** labeled *h*NAAA in cell extracts, and this effect was blocked by incubation with **4** (Figure 3 C). In contrast, incubation with **8** only partially antagonized *h*NAAA labeling by **5** and at short incubation times (Figure 3 C). Lastly, kinetic analyses revealed that **8**
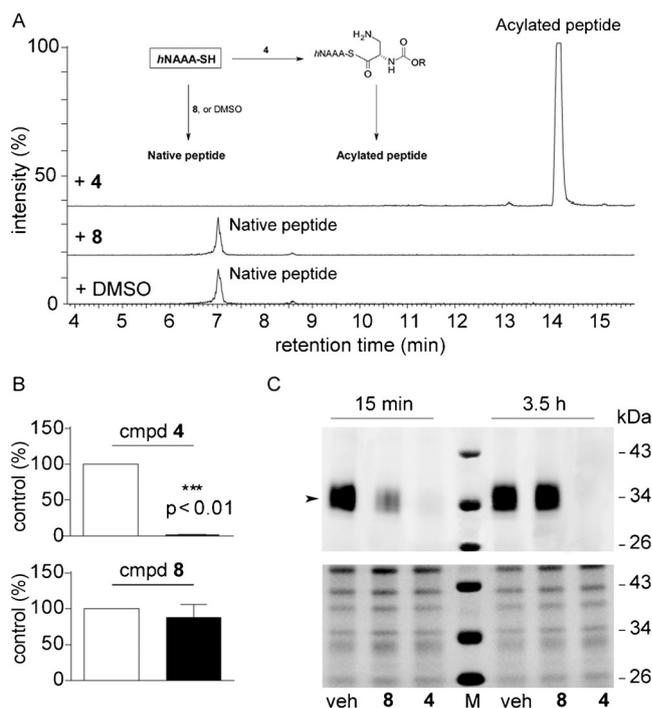
Figure 3. Compound **8** inhibits NAAA by a non-covalent mechanism. A) LC-MS tracings showing (top) that the covalent inhibitor **4** forms an adduct with a peptide containing the catalytic C126 (C126TSIVAQDSR) of NAAA (see inset), whereas (bottom) **8** or its vehicle (DMSO) have no such effect. B) Covalent inhibitor **4** (top) or **8** (bottom) was incubated with NAAA (filled bars) or buffer alone (open bars) and quantified in supernatant after protein precipitation. Bars: mean ± SEM, n = 3. C) Lysosomal extracts of *h*NAAA-overexpressing HEK293 cells were incubated with vehicle (2% DMSO), **4** or **8**, for 2 h before addition of probe **5**. A rhodamine fluorophore was inserted by click chemistry. The arrowhead indicates NAAA. Fluorescence (top), Coomassie Blue staining (loading control; bottom).
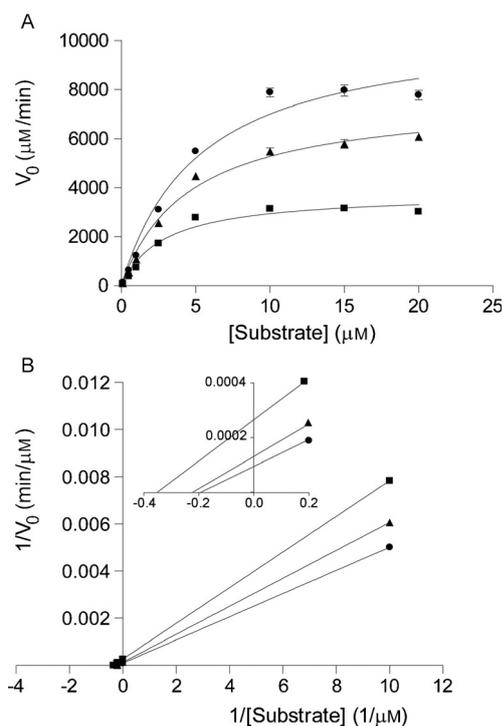
Figure 4. A) Michaelis–Menten analysis of the reaction of *h*NAAA in the presence of vehicle (DMSO, ——●——) or **8** (50 nM, ——▲——; 200 nM, ——■——). B) Lineweaver–Burk plot indicates uncompetitive inhibition (inset: magnification of the plot close to its origin).

Figure 5. PK and pharmacodynamic profiles of **8** in mice. A) Levels of **8** in the plasma (——●——) or brain (——▲——) after oral administration (3 mg kg⁻¹). B) Time course of the effects of **8** (30 mg kg⁻¹) on PEA, OEA, and anandamide (AEA) levels in the brain. Results are expressed as mean ± SEM, $n = 3$. * $P < 0.05$; **, $P < 0.01$; ***, $P < 0.001$, one-way ANOVA.

inhibits NAAA by an uncompetitive mechanism (Figure 4 A,B). The results identify **8** as the first non-covalent NAAA inhibitor disclosed to date.

The unprecedented mechanistic profile of **8** prompted us to test the compound's usefulness as an oral agent. In vitro studies demonstrated that **8** is soluble in aqueous buffer (pH 7.4) and stable in mouse plasma (Table 5). Similarly, **8** is stable in mouse liver microsomes (MLM).

Experiments in mice showed that **8** is extensively absorbed after oral administration (Figure 5 A). The pharmacokinetic (PK) parameters listed in Table 5 indicate that **8** had excellent oral bioavailability. Importantly, **8** crossed the blood–brain barrier, reaching a brain-to-plasma ratio of 0.2 and causing a substantial accumulation of PEA and OEA in brain tissue (Figure 5 A,B). No changes were seen in the levels of the anandamide, an endocannabinoid lipid amide that is degraded by fatty acid amide hydrolase (FAAH) rather than by NAAA.[3]

A selectivity screen showed that **8** (10 μM) had little or no effect on a panel of more than 50 receptors, ion channels, and transporters (Supporting Information, Table S2). Moreover, as expected from our target engagement studies (Figure 5 B), **8** had only a weak inhibitory effect on FAAH (IC₅₀ ≈ 10 μM),[10] and no effect on either acid ceramidase (a cysteine amidase that has 33–34 % identity with NAAA)[1] or monoacylglycerol lipase (a serine hydrolase that degrades the endocannabinoid 2-arachidonoyl-*sn*-glycerol).[11]

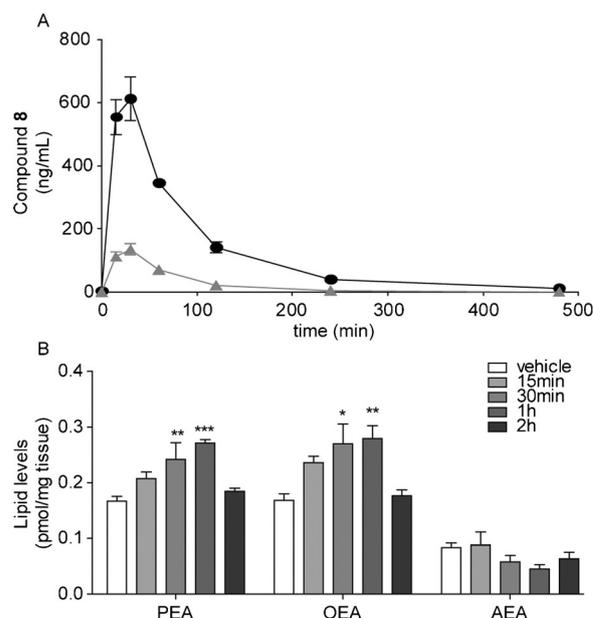MS is a neuroinflammatory disorder accompanied by alterations in cerebrospinal and plasma levels of PEA and

OEA.[12] PEA administration attenuates spasticity in the experimental allergic encephalomyelitis (EAE) model of MS.[13] Consequently, we tested whether accrual of PEA/OEA by treatment with **8** might be beneficial in this model. EAE mice and sham-immunized controls were treated with **8** (30 mg kg⁻¹, twice daily) or vehicle for 28 days, while recording clinical scores and body weight gain. Clinical scores were generated using a symptom scale that ranged from 0 (no clinical signs) to 5 (moribund).[14]

Figure 6 shows that treatment with **8** did not affect sham-immunized mice, whereas it delayed disease onset, attenuated symptom intensity, and normalized body weight in EAE animals. Moreover, **8** reduced mononuclear cell infiltration and microglia activation—two anatomical correlates of disease—in the spinal cord of EAE mice (Supporting Information, Figure S2). Further underscoring the superiority of **8** relative to known NAAA inhibitors, the highly potent covalent β-lactam derivative **4** had no effect in the EAE model (Supporting Information, Figure S3).

In summary, the present study describes a novel class of benzothiazole–piperazine derivatives that inhibit NAAA by a non-covalent, uncompetitive mechanism. A representative member of this class, **8**, shows excellent oral PK properties and good brain penetration. The strong protective activity of **8** in a mouse model of MS is similar to those of other agents used to target this disease.[15] Compound **8** exemplifies a new generation of non-covalent NAAA inhibitors that may find therapeutic applications in the treatment of neuro-inflammation.
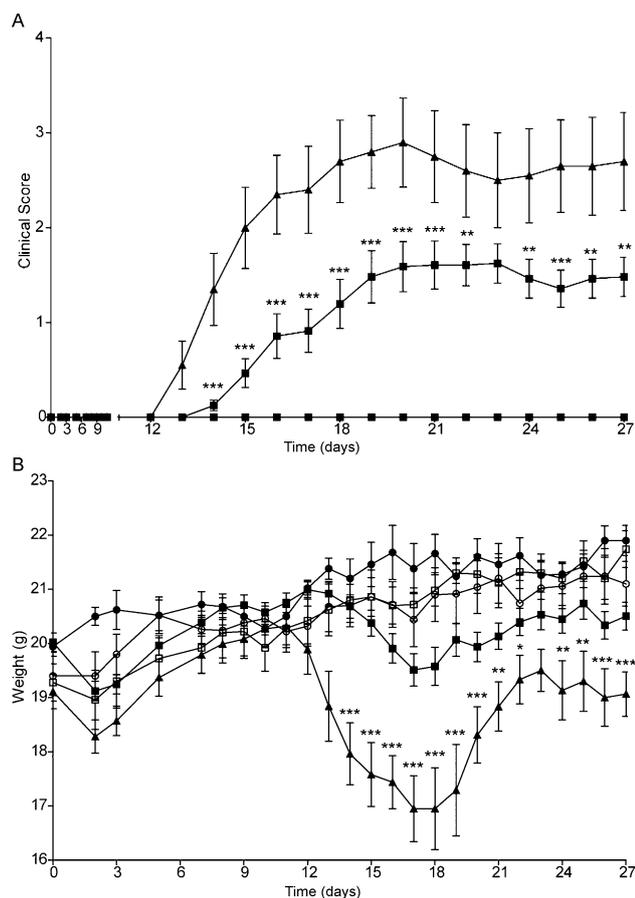
Figure 6. Time-course of the effects of **8** or vehicle on A) clinical score and B) body weight in EAE mice and sham-immunized controls. **8** was administered at 30 mg kg^{-1} twice daily. MOG: myelin oligodendrocyte glycoprotein 35–55, antigen used to induce EAE. Results are expressed as mean ± SEM, $n = 30$. * $P < 0.05$; **, $P < 0.01$; ***, $P < 0.001$, two-way ANOVA followed by Bonferroni post hoc test. Key: MOG(+)+veh (——▲——); MOG(+)+**8** (——■——); MOG(−)+veh (——□——); MOG(−)+**8** (——○——); Naive (——●——).

Acknowledgements

[1] a) K. Tsuboi, Y. X. Sun, Y. Okamoto, N. Araki, T. Tonai, N. Ueda, *J. Biol. Chem.* **2005**, *280*, 11082–11092; b) K. Tsuboi, N. Takezaki, N. Ueda, *Chem. Biodiversity* **2007**, *4*, 1914–1925; c) N. Ueda, K. Tsuboi, T. Uyama, *Prog. Lipid Res.* **2010**, *49*, 299–315.
[2] S. Pontis, A. Ribeiro, O. Sasso, D. Piomelli, *Crit. Rev. Biochem. Mol. Biol.* **2016**, *51*, 7–14.
[3] D. Piomelli, O. Sasso, *Nat. Neurosci.* **2014**, *17*, 164–174.
[4] T. Bandiera, S. Ponzano, D. Piomelli, *Pharmacol. Res.* **2014**, *86*, 11–17.
[5] a) A. Armirotti, E. Romeo, S. Ponzano, L. Mengatto, M. Dionisi, C. Karacsonyi, F. Bertozzi, G. Garau, G. Tarozzo, A. Reggiani, T. Bandiera, G. Tarzia, M. Mor, D. Piomelli, *ACS Med. Chem. Lett.* **2012**, *3*, 422–426; b) A. Ribeiro, S. Pontis, L. Mengatto, A. Armirotti, V. Chiurchiu, V. Capurro, A. Fiasella, A. Nuzzi, E. Romeo, G. Moreno-Sanz, M. Maccarrone, A. Reggiani, G. Tarzia, M. Mor, F. Bertozzi, T. Bandiera, D. Piomelli, *ACS Chem. Biol.* **2015**, *10*, 1838–1846.
[6] A. Duranti, A. Tontini, F. Antonietti, F. Vacondio, A. Fioni, C. Silva, A. Lodola, S. Rivara, C. Solorzano, D. Piomelli, G. Tarzia, M. Mor, *J. Med. Chem.* **2012**, *55*, 4824–4836.
[7] a) A. Ariza, C. Mayorga, T. D. Fernandez, N. Barbero, A. Martin-Serrano, D. Perez-Sala, F. J. Sanchez-Gomez, M. Blanca, M. J. Torres, M. I. Montanez, *J. Invest. Allergol. Clin. Immunol.* **2015**, *25*, 12–25; b) I. Karlsson, K. Samuelsson, D. J. Ponting, M. Tornqvist, L. L. Ilag, U. Nilsson, *Sci. Rep.* **2016**, *6*, 21203.
[8] M. Alhouayek, P. Bottemanne, K. V. Subramanian, D. M. Lambert, A. Makriyannis, P. D. Cani, G. G. Muccioli, *FASEB J.* **2015**, *29*, 650–661.
[9] E. Romeo, S. Ponzano, A. Armirotti, M. Summa, F. Bertozzi, G. Garau, T. Bandiera, D. Piomelli, *ACS Chem. Biol.* **2015**, *10*, 2057–2064.
[10] K. Ahn, M. K. McKinney, B. F. Cravatt, *Chem. Rev.* **2008**, *108*, 1687–1707.
[11] J. L. Blankman, G. M. Simon, B. F. Cravatt, *Chem. Biol.* **2007**, *14*, 1347–1356.
[12] a) M. Di Filippo, L. A. Pini, G. P. Pelliccioli, P. Calabresi, P. Sarchielli, *J. Neurol. Neurosurg. Psychiatry* **2008**, *79*, 1224–1229; b) L. Jean-Gilles, S. Feng, C. R. Tench, V. Chapman, D. A. Kendall, D. A. Barrett, C. S. Constantinescu, *J. Neurol. Sci.* **2009**, *287*, 212–215.
[13] D. Baker, G. Pryce, J. L. Croxford, P. Brown, R. G. Pertwee, A. Makriyannis, A. Khanolkar, L. Layward, F. Fezza, T. Bisogno, V. Di Marzo, *FASEB J.* **2001**, *15*, 300–302.
[14] I. M. Stromnes, J. M. Goverman, *Nat. Protoc.* **2006**, *1*, 1810–1819.
[15] a) J. W. Choi, S. E. Gardell, D. R. Herr, R. Rivera, C. W. Lee, K. Noguchi, S. T. Teo, Y. C. Yung, M. Lu, G. Kennedy, J. Chun, *Proc. Natl. Acad. Sci. USA* **2011**, *108*, 751–756; b) H. Deng, S. G. Bernier, E. Doyle, J. Lorusso, B. A. Morgan, W. F. Westlin, G. Evindar, *ACS Med. Chem. Lett.* **2013**, *4*, 942–947; c) H. Chen, J. C. Assmann, A. Krenz, M. Rahman, M. Grimm, C. M. Karsten, J. Kohl, S. Offermanns, N. Wettschureck, M. Schwaninger, *J. Clin. Invest.* **2014**, *124*, 2188–2192.